

## Laser Shaping of a Relativistic Intense, Short Gaussian Pulse by a Plasma Lens

H. Y. Wang,<sup>1</sup> C. Lin,<sup>1,\*</sup> Z. M. Sheng,<sup>2</sup> B. Liu,<sup>1</sup> S. Zhao,<sup>1</sup> Z. Y. Guo,<sup>1</sup> Y. R. Lu,<sup>1</sup> X. T. He,<sup>1</sup> J. E. Chen,<sup>1</sup> and X. Q. Yan<sup>1,†</sup>

<sup>1</sup>State Key Laboratory of Nuclear Physics and Technology, Peking University, Beijing 100871, China, and Key Lab of High Energy Density Physics Simulation, CAPT, Peking University, Beijing 100871, China

<sup>2</sup>Key Laboratory for Laser Plasmas (MoE) and Department of Physics, Shanghai Jiao Tong University, Shanghai 200240, China and Beijing National Laboratory of Condensed Matter Physics, Institute of Physics, CAS, Beijing 100190, China

(Received 17 September 2011; published 22 December 2011)

By 3D particle-in-cell simulation and analysis, we propose a plasma lens to make high intensity, high contrast laser pulses with a steep front. When an intense, short Gaussian laser pulse of circular polarization propagates in near-critical plasma, it drives strong currents of relativistic electrons which magnetize the plasma. Three pulse shaping effects are synchronously observed when the laser passes through the plasma lens. The laser intensity is increased by more than 1 order of magnitude while the initial Gaussian profile undergoes self-modulation longitudinally and develops a steep front. Meanwhile, a nonrelativistic prepulse can be absorbed by the overcritical plasma lens, which can improve the laser contrast without affecting laser shaping of the main pulse. If the plasma skin length is properly chosen and kept fixed, the plasma lens can be used for varied laser intensity above  $10^{19}$  W/cm<sup>2</sup>.

DOI: 10.1103/PhysRevLett.107.265002

PACS numbers: 52.38.Kd, 41.75.Jv, 52.35.Mw, 52.59.-f

The recent development of ultrashort-pulse high peak power laser systems enables us to investigate high field science under extreme conditions [1], which opened new and active research fields such as fast ignition of inertial confinement fusion [2], laboratory astrophysics [3], and development of a compact source of high-energy electrons and ions [4].

Generation of high-energy ions by ultraintense laser pulses has been intensively studied due to its wide range of applications [5,6]. Radiation pressure acceleration has been proposed as a promising route to obtain high-quality ion beams in a much more efficient way [7–13], compared to the target normal sheath acceleration [14–16]. In order to accelerate ions to a relativistic velocity in the radiation pressure acceleration regime, hole-boring effects [10] and transverse instabilities [17] should be restrained, which normally require extremely high laser intensity ( $> 10^{21}$  W/cm<sup>2</sup>), a sharp rising front, and high temporal laser contrast ( $> 10^{10}$ ). Such a laser pulse is also promising for attosecond UV and x-ray sources from plasma surfaces of solid foil [18].

In this Letter we report on a laser-driven plasma lens that can transversely focus the laser beam to the sublaser wavelength in the radius and enhance the laser intensity by more than 1 order of magnitude, while temporally steepening the Gaussian pulse and improving the laser contrast. One fundamental nonlinear effect of laser-plasma interaction arises from the relativistic motion of the electrons in the intense laser field [19]. In particular, the transverse and axial profiles of the laser pulse can be changed by relativistic self-focusing (RSF) [20] and relativistic self-phase modulation (RSPM) [21]. Laser shaping by nonlinear interactions of an intense pulse in underdense plasma is discussed by weekly nonlinear theory and simulations

[22]. The RSF of a linearly polarized laser beam in a near-critical plasma has been investigated by Pukhov and Meyer-ter-Vehn, which shows that the magnetic interaction plays an important role during RSF in the 3D simulations [23]. For near-critical plasma, the Raman instability that otherwise destroys the pulse is prohibited. RSPM can be very effective in this density region and results in a smooth pulse self-compression [24]. For relativistically strong ( $|a| \geq 1$ ) laser pulses, however, the weak nonlinearity approximation is not valid anymore, because the nonlinear interactions can be rather complex and must be understood in conjunction with generation of a strongly nonlinear wakefield, erosion of the leading edge, and generation of the quasistatic magnetic field, etc. [1]. By means of 3D simulations we found that RSF, RSPM, and relativistic transparency effects are dynamically related together in laser interaction with the near-critical plasma. The laser pulse is focused to a smallest spot size and the focused intensity can be increased by a factor of 25. At the same time the initial Gaussian pulse becomes steepened, meanwhile a nonrelativistic prepulse can be absorbed by the overcritical plasma and the laser contrast is improved. For the proper chosen plasma lens parameters, the three lens effects above are effective for varied laser intensity above  $10^{19}$  W/cm<sup>2</sup>. Therefore the plasma slab can be used as a plasma lens to generate high intensity, high contrast, and steepened laser pulses, which is quite challenging for state of the art laser technology.

In the relativistic regime magnetic interaction appears to be due to the fact that electrons accelerated inside a self-focused laser pulse produce electric currents in the plasma and an associated quasistatic magnetic field. The electron velocity is limited by the velocity of light in vacuum, so the electron current density is approximately equal to  $en_e c$ ,

where  $e, n_e$ , and  $c$  is the charge of electron, electron density, and speed of light in vacuum, respectively. Omitting the numerical factors, the quasistatic magnetic field at the distance  $r$  from the axis reads:

$$B_s = (en_e)2\pi r. \quad (1)$$

For a uniform plasma, the self-generated magnetic field vanishes at the channel axis and reaches a maximum at the channel edges. The quasistatic magnetic field pinches the relativistic electrons into a channel with a radius  $r$  assumed to equal the diameter of Larmor motion in quasimagnetic field  $B_s$ , which has been testified in 3D simulation later.

$$r = 2\gamma mc^2/eB_s, \quad (2)$$

where  $\gamma = \sqrt{a^2 + 1} \sim a$  for  $a \gg 1$ . Here  $a = eE_L/m_e\omega c$  is the normalized vector potential for a laser with electric field  $E_L$  and laser frequency  $\omega$ . Combining Eqs. (1) and (2) we have:

$$r = \frac{1}{\pi} \sqrt{an_c/n_e} \lambda, \quad (3)$$

and then we obtain the magnetic field:

$$B_s = \sqrt{an_e/n_c} B_0, \quad (4)$$

where  $B_0 = m_e c \omega / e$ . For the light of wavelength  $\lambda = 2\pi c / \omega = 1 \mu\text{m}$ , one obtains  $B_0 = 107.1 \text{ MG}$ . The electric currents leads to a redistribution of fast electrons, which in turn changes the refractive index  $\eta = [1 - \omega_p^2/(\gamma\omega^2)]^{1/2}$ . As the laser has a Gaussian profile, the index of refraction is peaked along the propagation axis. The phase velocity  $v_p = c/\eta$  is smaller on axis than off axis and RSF occurs. As  $v_p v_g = c^2$ , the group velocity of the laser pulse vertex is larger than the pulse front, which causes the RSPM process. These two processes and pinch effects of the magnetic field  $B_s$  exist in the laser-plasma interactions, which can reshape the laser profile in both transverse and longitudinal directions.

To illustrate specific features of the laser shaping in three-dimensional regimes, we carried out 3D simulations using a fully relativistic particle-in-cell code (KLAP3D) [9,25]. The simulation box is  $60\lambda \times 20\lambda \times 20\lambda$  and contains  $600 \times 200 \times 200$  cells. A circularly polarized laser pulse with a Gaussian envelope  $a = a_0 \exp[-(y - y_0)^2/r_0^2] \exp[-(x - x_0)^2/r_0^2] \exp[-(t - t_0)^2/\tau^2]$  in both the longitudinal ( $z$ ) and transverse ( $x, y$ ) directions is normally incident from the left side ( $z = 0 \mu\text{m}$ ). We shall set  $a_0 = 16.5$ , corresponding to a peak laser intensity of  $7.46 \times 10^{20} \text{ W cm}^{-2}$ ,  $t_0 = 50 \text{ T}$ ,  $\tau = 25 \text{ T}$ ,  $r_0 = 6\lambda$ ,

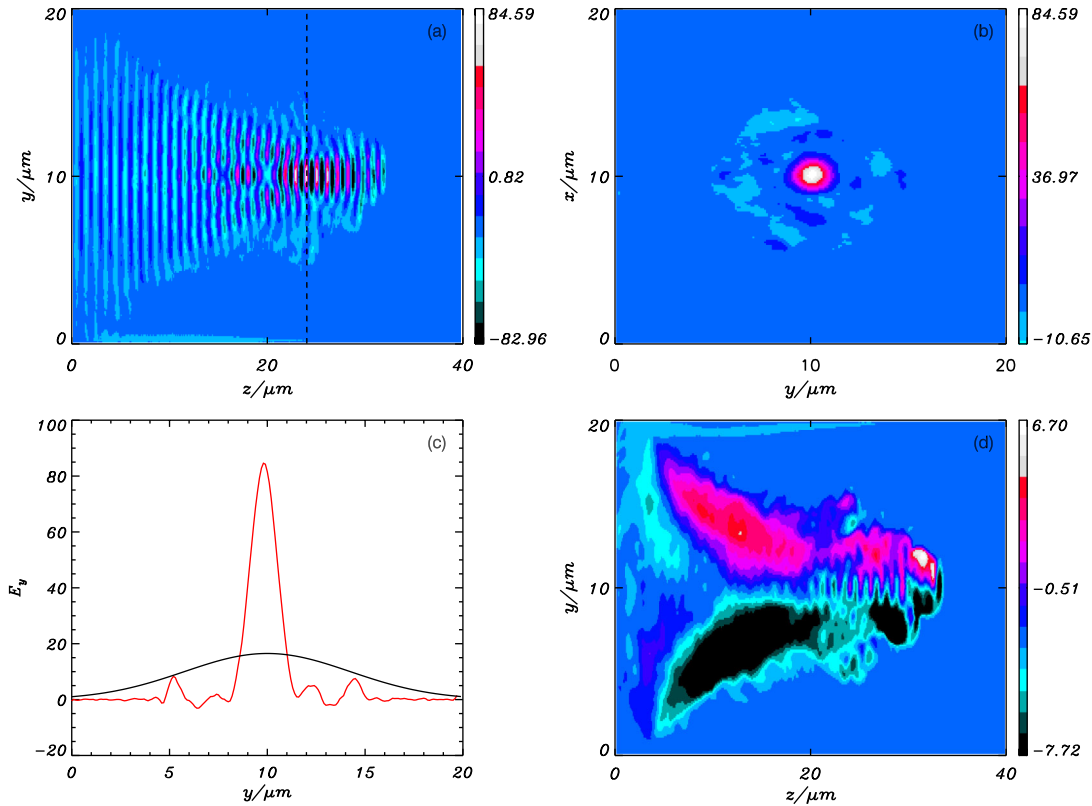


FIG. 1 (color online). Transverse pulse self-focusing at  $t = 72 \text{ T}$ : (a) ( $Z, Y$ ) section of  $E_y$  at  $x = 10 \mu\text{m}$  (in units of  $m_e c \omega / e$ ), the dashed line marks transverse sections shown in (b),(c); (b) ( $X, Y$ ) section of  $E_y$  at  $z = 24.1 \mu\text{m}$ ; (c)  $E_y$  along  $y$  axis at  $z = 24.1 \mu\text{m}$ ,  $x = 10 \mu\text{m}$ , the black line shows the initial laser transverse profile. (d) ( $Z, Y$ ) section of quasistatic magnetic field  $B_x$  (in units of  $m_e \omega / e$ ) at  $t = 72 \text{ T}$ , averaged over 2 laser periods.

$y_0 = 10\lambda$  and  $x_0 = 10\lambda$ , where  $T = 3.3$  fs is the laser period. The uniform carbon plasma of density  $n_0 = 2.4n_c$  is placed between  $3\lambda \leq z \leq 60\lambda$ , where  $n_c$  is the critical plasma density. Each cell is filled with 8 quasiparticles. The initial temperature of the electrons and carbon ions is 5 eV.

The transverse pulse self-focusing process at  $t = 72$  T is shown in Fig. 1. The incident beam first propagates through an unstable filamentary stage and then collapses into a single channel as shown in Fig. 1(a). The laser pulse is focused to a smallest spot size at  $z = 24.1 \mu\text{m}$ , corresponding to a laser self-focusing length of about  $21.1 \mu\text{m}$ . The normalized electric field  $E_y$  is 84.59 which is increased by a factor of 5 and the laser intensity is 25 times higher than the initial one. The  $(X, Y)$  section of  $E_y$  in Fig. 1(b) shows that the pulse self-focusing process is symmetrical. The laser retains its Gaussian radial profile within the channel with a radius of about  $0.9\lambda$  as seen in Fig. 1(c), which is in good agreement with Equation. (3) (theory predicts  $0.83\lambda$ ). The coalescence of the filaments by magnetic interaction are well explained on the basis of the magnetic interaction by Askaryan *et al.* [26]. In Fig. 1(d), the  $(Z, Y)$  section of the quasistatic magnetic field  $B_x$  averaged over 2 laser periods is plotted. This field vanishes at the channel axis and reaches a maximum at the edges. The maximum magnetic field is about 6.7 at the edges, which agrees well with the theoretical prediction of 6.29 by Eq. (4).

Figure 2 shows how the pulse profile changes in the longitudinal direction by laser compression during its propagation through different plasma planes. It shows an efficient laser compression at  $z = 24.1 \mu\text{m}$ , where the laser propagates a plasma slab length that is the same as the self-focusing length. At the same time the laser pulse developed a steep front of about 8 T. This implies that a initial Gaussian profile is nearly transformed into a quasi-step function pulse. For a plasma length longer or shorter

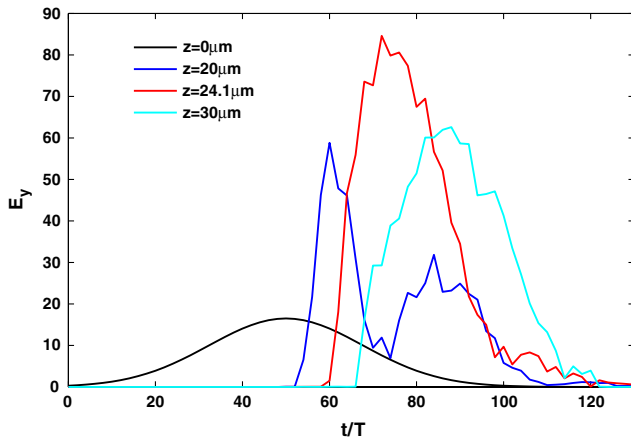


FIG. 2 (color online). Longitudinal pulse compression: On-axis envelope profile  $E_y$  at  $z = 0 \mu\text{m}$ ,  $z = 20 \mu\text{m}$ ,  $z = 24.1 \mu\text{m}$ , and  $z = 30 \mu\text{m}$ .

than the self-focusing length, the laser compression is less efficient.

We now study the optimistic parameters for the plasma lens. Considering laser shaping of an intense laser pulse, three typical parameters are critical for the process: (i) increase of the normalized vector potential on axis  $f_0 = a_{\text{max}}/a_0$ ; (ii) laser rise time  $r_T$ ; (iii) laser transmission efficiency  $t_E$ . Figure 3(a) shows the influence of plasma density on these three parameters with  $a_0 = 16.5$ . The normalized vector potential on axis can be enhanced by a factor of 5 for plasma density varied from  $1n_c$  to  $5n_c$ . We should note that the laser transmission efficiency  $t_E$  decreases with plasma density increasing, while the laser rise time  $r_T$  decreases rapidly to about 8 T at  $n_e = 2.4n_c$  and becomes saturated. The laser transmission efficiency is about 30% at this point while it can be as high as 60% with plasma density of  $n_e = 1.5n_c$  if the pulse rise time can be compromised. The quasistatic magnetic field  $B_s$  and the channel radius  $r$  observed in simulation are consistent with the theoretical value from Eqs. (3) and (4) as shown in Figs. 3(b) and 3(d). For a fixed plasma skin length  $l_s/\lambda = \sqrt{an_c/n_e} = 2.6$ , the enhancement of laser amplitude, laser rise time, transmission, and the channel radius  $r$  are nearly the same for varied laser intensity ranging from  $10^{19}$  W/cm<sup>2</sup> to  $10^{21}$  W/cm<sup>2</sup> as shown in Figs. 3(c) and 3(d).

This means that the plasma lens works for different laser intensities when keeping the plasma skin length fixed. As a result, if we choose a proper plasma density (satisfy  $l_s/\lambda \sim 2.6$ ) and a proper plasma slab length (equal the self-focusing length), the laser focusing and compressing can be realized at the same time and same position. This provides an efficient way to generate a high intensity laser pulse with a sharp rising front by laser shaping in both the transverse and longitudinal directions.

The improvement of the laser pulse contrast (the intensity ratio between the main pulse and the prepulse) is

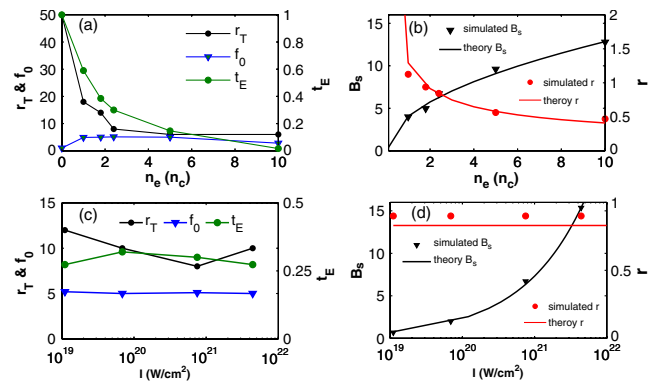


FIG. 3 (color online). Pulse shaping for varied plasma density and laser intensity (a)  $f_0$ ,  $r_T$  and  $t_E$  for varied plasma density at  $a_0 = 16.5$ ; (b)  $B_s$  and  $r$  for varied plasma density at  $a_0 = 16.5$ ; (c)  $f_0$ ,  $r_T$  and  $t_E$  for varied laser intensity with fixed plasma skin length  $l_s/\lambda = \sqrt{an_c/n_e} = 2.6$ ; (d)  $B_s$  and  $r$  for varied laser intensity with fixed plasma skin length  $l_s/\lambda = \sqrt{an_c/n_e} = 2.6$ .

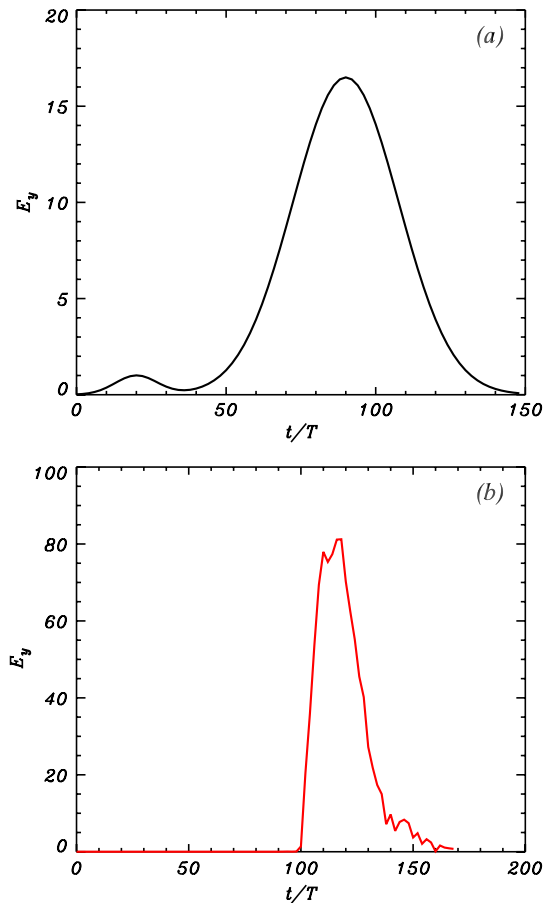


FIG. 4 (color online). Absorbing of laser prepulse: (a) On-axis envelope profile  $E_y$  at  $z = 0 \mu\text{m}$ ; (b) On-axis envelope profile  $E_y$  at  $z = 24.1 \mu\text{m}$ .

promising for various applications. Relativistic transparency provides a way to achieve laser pulse shaping and generate a high contrast laser pulse [27]. In particle-in-cell (PIC) simulations here, we study the prepulse absorbing process. We set a prepulse of  $a = 1$ ,  $\tau = 10 T$  and  $r_0 = 6\lambda$ , which is 40 T before the main pulse as shown in Fig. 4(a). It is observed that the prepulse can be absorbed in the plasma without affecting the shaping of the main pulse as shown in Fig. 4(b). This shows the plasma lens can also improve the contrast of laser pulse.

In summary we propose a scheme to make a high intensity laser pulse with a high contrast and a steep rise front using a plasma lens. As relativistic self-focusing (RSF), relativistic self-phase modulation (RSPM) and relativistic transparency are dynamically related together in laser interaction with the near-critical plasma, the lens has three shaping effects: (I) pulse focusing that results in laser intensity enhancement; (II) laser profile steepening that can transform a Gaussian pulse into a quasistep function pulse; (III) absorption of nonrelativistic prepulse. The transmission efficiency of the lens can be as high as 60%. The generated laser pulse should be useful for many

applications such as generation of high-energy ions and electrons. The optimistic lens parameter (plasma skin length) is determined in 3D simulations. This scheme has no limitation for laser intensity above  $10^{19} \text{ W/cm}^2$ , since it involves only laser-plasma interaction.

This work was supported by the National Natural Science Foundation of China (Grants No. 10935002, No. 10835003, and No. 11025523) and the National Basic Research Program of China (Grant No. 2011CB808104).

\*linchen\_0812@pku.edu.cn

†x.yan@pku.edu.cn

- [1] G. A. Mourou *et al.*, *Rev. Mod. Phys.* **78**, 309 (2006).
- [2] M. Roth *et al.*, *Phys. Rev. Lett.* **86**, 436 (2001); V. Yu. Bychenkov *et al.*, *Plasma Phys. Rep.* **27**, 1017 (2001); S. Atzeni *et al.*, *Nucl. Fusion* **42**, L1 (2002).
- [3] B. A. Remington *et al.*, *Science* **284**, 1488 (1999); S. V. Bulanov *et al.*, *Eur. Phys. J. D* **55**, 483 (2009).
- [4] T. Tajima and J. M. Dawson, *Phys. Rev. Lett.* **43**, 267 (1979); E. Esarey, C. B. Schroeder, and W. P. Leemans, *Rev. Mod. Phys.* **81**, 1229 (2009); S. P. Hatchett *et al.*, *Phys. Plasmas* **7**, 2076 (2000); E. L. Clark *et al.*, *Phys. Rev. Lett.* **84**, 670 (2000); A. Maksimchuk *et al.*, *ibid.* **84**, 4108 (2000); A. McPherson *et al.*, *Nature (London)* **370**, 631 (1994).
- [5] M. Borghesi *et al.*, *Phys. Plasmas* **9**, 2214 (2002).
- [6] S. V. Bulanov *et al.*, *Phys. Lett. A* **299**, 240 (2002); T. Zh. Esirkepov *et al.*, *Phys. Rev. Lett.* **89**, 175003 (2002).
- [7] S. S. Bulanov *et al.*, *Med. Phys.* **35**, 1770 (2008); B. Eliasson *et al.*, *New J. Phys.* **11**, 073006 (2009); A. Macchi, S. Veghini, and F. Pegoraro, *Phys. Rev. Lett.* **103**, 085003 (2009); Z. M. Zhang *et al.*, *Phys. Plasmas* **17**, 043110 (2010); T. Esirkepov *et al.*, *Phys. Rev. Lett.* **92**, 175003 (2004); A. Henig *et al.*, *Phys. Rev. Lett.* **103**, 045002 (2009); S. G. Rykovanov *et al.*, *New J. Phys.* **10**, 113005 (2008); C. S. Liu *et al.*, *AIP Conf. Proc.* **1061**, 246 (2008).
- [8] X. Zhang *et al.*, *Phys. Plasmas* **14**, 123108 (2007).
- [9] X. Q. Yan *et al.*, *Phys. Rev. Lett.* **100**, 135003 (2008).
- [10] A. Macchi *et al.*, *Phys. Rev. Lett.* **94**, 165003 (2005).
- [11] O. Klimo *et al.*, *Phys. Rev. ST Accel. Beams* **11**, 031301 (2008).
- [12] A. P. L. Robinson *et al.*, *New J. Phys.* **10**, 013021 (2008).
- [13] M. Chen *et al.*, *Phys. Rev. Lett.* **103**, 024801 (2009); X. Q. Yan *et al.*, *Phys. Rev. Lett.* **103**, 135001 (2009); S. V. Bulanov *et al.*, *Phys. Rev. Lett.* **104**, 135003 (2010); B. Qiao *et al.*, *Phys. Rev. Lett.* **102**, 145002 (2009).
- [14] R. A. Snavely *et al.*, *Phys. Rev. Lett.* **85**, 2945 (2000).
- [15] H. Schworer *et al.*, *Nature (London)* **439**, 445 (2006); B. M. Hegelich *et al.*, *Nature (London)* **439**, 441 (2006); A. J. Mackinnon *et al.*, *Phys. Rev. Lett.* **88**, 215006 (2002); S. P. Hatchett *et al.*, *Phys. Plasmas* **7**, 2076 (2000); L. Willingale *et al.*, *Phys. Rev. Lett.* **96**, 245002 (2006); L. Robson *et al.*, *Nature Phys.* **3**, 58 (2006); A. Yogo *et al.*, *Phys. Rev. E* **77**, 016401 (2008).

- [16] J. Fuchs *et al.*, *Nature Phys.* **2**, 48 (2005).
- [17] F. Pegoraro and S. V. Bulanov, *Phys. Rev. Lett.* **99**, 065002 (2007).
- [18] C. D. Tsakiris *et al.*, *New J. Phys.* **8**, 19 (2006); Y. Nomura *et al.*, *Nature Phys.*, **5**, 124 (2008).
- [19] W. B. Mori, *IEEE J. Quantum Electron.* **33**, 1942 (1997), and references therein.
- [20] A. G. Litvak, *Zh. Eksp. Teor. Fiz.* **57**, 629 (1969) [*Sov. Phys. JETP* **30**, 344 (1970)]; P. Sprangle, C. M. Tang, and E. Esarey, *IEEE Trans. Plasma Sci.* **15**, 145 (1987); G.-Z. Sun *et al.*, *Phys. Fluids* **30**, 526 (1987); X. L. Chen and R. N. Sudan, *Phys. Rev. Lett.* **70**, 2082 (1993); E. Esarey *et al.*, *IEEE J. Quantum Electron.* **33**, 1879 (1997), and references therein.
- [21] C. Max, J. Arons, and A. B. Langdon, *Phys. Rev. Lett.* **33**, 209 (1974); C. J. Mackinstrie and R. Bingham, *Phys. Fluids B* **4**, 2626 (1992).
- [22] C. Ren *et al.*, *Phys. Rev. E* **63**, 026411 (2001); S. S. Bulanov *et al.*, *Phys. Plasmas* **17**, 043105 (2010).
- [23] A. Pukhov and J. Meyer-ter-Vehn, *Phys. Rev. Lett.* **76**, 3975 (1996).
- [24] O. Shorokhov, A. Pukhov, and I. Kostyukov, *Phys. Rev. Lett.* **91**, 265002 (2003).
- [25] Z. M. Sheng *et al.*, *Phys. Rev. Lett.* **94**, 095003 (2005).
- [26] G. A. Askar'yan *et al.*, *JETP Lett.* **60**, 251 (1994).
- [27] A. V. Vshivkov *et al.*, *Nucl. Instrum. Methods Phys. Res., Sect. A* **410**, 493 (1998); A. V. Vshivkov *et al.*, *Phys. Plasmas* **5**, 2727 (1998).